Two-wavelength laser diode interferometer with time-sharing sinusoidal phase modulation

Takamasa Suzuki, Takayuki Yazawa, and Osami Sasaki

We describe an interferometer system that uses two separate wavelengths to measure step height. The overlapping interference images detected by a CCD camera are easily separated by an ordinary integrating-bucket method and time-sharing sinusoidal phase modulation, in which two laser diodes are alternately modulated with a sinusoidal signal. A phase map is obtained only for the laser diode into which the modulation signal is injected. In this instance, a 1-μm step height was accurately detected. © 2002 Optical Society of America

OCIS codes: 120.3180, 120.3940, 120.5050, 120.5060, 120.6660, 140.2020.

1. Introduction

It is difficult for ordinary interferometers to measure a step shape whose height is greater than one half of one wavelength, but two-wavelength interferometers[1-3] (TWIs) can do so. In these conventional TWIs, however, separating interference signals is a complicated procedure. In a phase-shifting TWI,[3] for instance, illumination is switched from one wavelength to another wavelength in an alternating sequence. It is a time-consuming process. Also, multiple laser diode (LD) setups, which previously had attracted some attention, share one notable problem: how best to separate interference signals generated by two independent LDs. Whereas one can easily detect a single interference signal by shutting off the bias current of the second LD,[4] the latter device will suffer some damage from the sudden change. Also, it is not easy to modulate LDs with high frequency because the bias current becomes lower than the threshold current when the LD is shut off.

Moreover, although such interference signals can be detected and separated by polarization,[5] interference filters,[6] or the heterodyne technique,[7] multiple photodiodes (PDs) will be required. At present we can use only one PD for processing transient inter-ference, because individual signals are separated according to the time-multiplexed modulating signal,[8] the modulating frequency,[9] or the initial phase of the modulating signal,[10] in which case the PD is used for temporal signal processing, and real-time signal processing can be implemented. The PD or object, however, must be scanned mechanically with for a two-dimensional surface-profile measurement. This is a time-consuming process.

In this paper we describe a TWI that uses the integrating-bucket method in conjunction with our new modulating technique. A CCD image sensor is ideal for gauging two-dimensional surface profiles because no mechanical scan is required and the sensor can easily be linked with a computer. The Fourier-transform method was applied to a TWI that uses a CCD image sensor.[11] Interference fringes were separated with respect to each spatial frequency that depends on the wavelength and the tilt of a reference mirror. This technique, however, requires a time-consuming calculation of the Fourier transform. Thus the bucket method[12,13] is one of the best measurement techniques when a CCD image sensor is used as the photodetector. This method requires only simple operation and calculation of an arctan function. If we prepare a lookup table for the arctan function, the calculation time can be reduced significantly. Our technique of time-shared sinusoidal phase modulation enables us to separate the overlapped interference fringes by using the bucket method. A separate phase distribution is given only for a phase-modulated LD in our technique. As of this writing, a step height of 1 μm has been measured by our system with an accuracy of 15 nm rms.
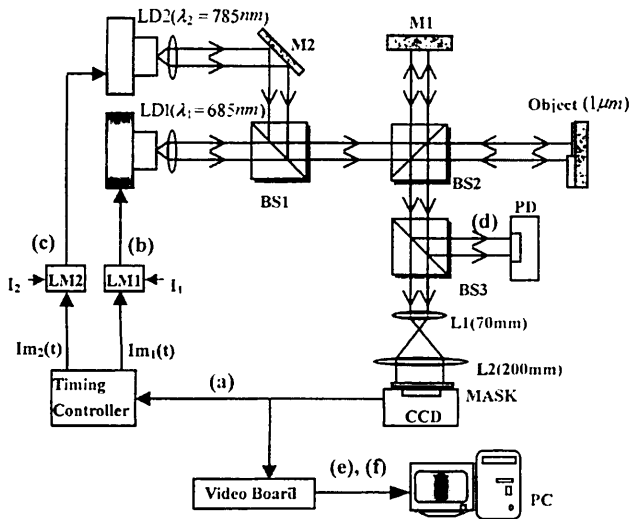
Fig. 1. Schematic of the experimental setup for a two-wavelength LD interferometer that uses time-sharing sinusoidal phase-modulation: M1, M2, mirrors; BS2, BS3, beam splitters; L1, L2, lenses; PC, personal computer; other abbreviations defined in text.

2. Principle

A. Optical Setup

The optical setup is shown in Fig. 1. Laser beams radiated from LD1 and LD2 fuse within beam splitter BS1. From there, they are fed into a Twyman–Green interferometer. The object consists of the three gauge blocks shown in Fig. 2. LD modulators LM1 and LM2 mix bias and modulating currents for LD1 and LD2, respectively, as shown in Fig. 1. I_1 and I_2 represent the dc bias currents employed. When sinusoidal modulating currents

$$\text{Im}_i(t) = m_i \cos(\omega_c t + \theta) \qquad (i = 1, 2) \qquad (1)$$

are used, the interference signals generated by the beams emanating from LD1 and LD2 are given by

$$S_i(t, x, y) = a_i(x, y) + b_i(x, y)\cos[z_i \cos(\omega_c t + \theta) + \alpha_i(x, y)] \qquad (i = 1, 2), \qquad (2)$$
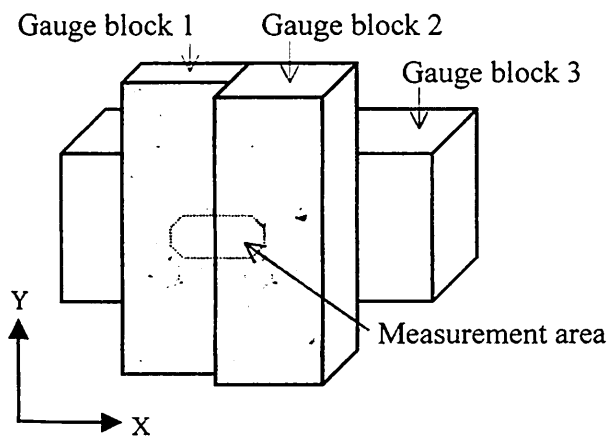

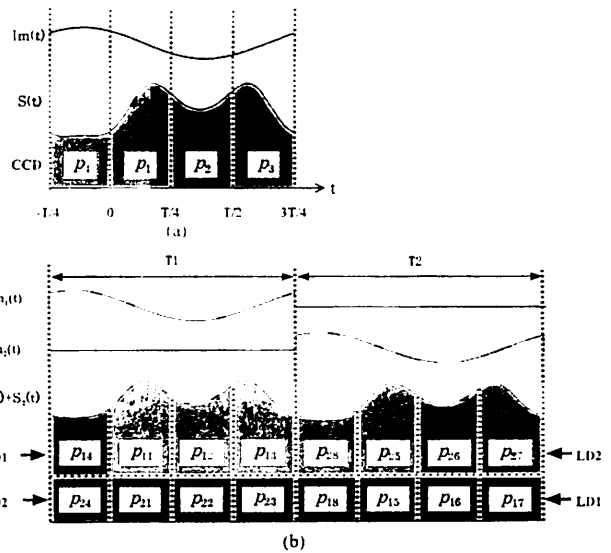Fig. 2. Test surface made from gauge blocks.

Fig. 3. Timing chart of integrating-bucket method for measuring profile with (a) the ordinary modulating technique and (b) time-sharing sinusoidal phase modulation.

where

$$z_i = 2\pi m_i \beta_i L_0 / \lambda_i^2 \qquad (i = 1, 2) \qquad (3)$$

represents modulation depths as determined by optical pass difference L_0 and

$$\alpha_i(x, y) = 4\pi L(x, y) / \lambda_i \qquad (i = 1, 2) \qquad (4)$$

are phase distributions related to the surface profile of $L(x, y)$. $\beta_i = \partial \lambda_i / \partial \text{Im}_i$ represents the modulation efficiency of the LD. The temporal interference signal can be monitored by a PD.

B. Bucket Method of Profilometry

The integrating-bucket method[12] is not only a simple but also a powerful technique for measuring profiles with a CCD image sensor. A schematic explanation of this method is shown in Fig. 3. We explain it as simply as possible by focusing our attention on a single interference signal, as shown in Fig. 3(a). Images detected by a CCD image sensor are given as temporally integrated values of the incident interference signal. When the charge-storage period is set to one quarter of a modulating period, we are able to detect four separate images,

$$p_i(x, y) = \int_{(T/4)(i-1)}^{(T/4)i} S(t, x, y) dt \qquad (i = 1\text{--}4), \qquad (5)$$

during modulation. Then, by simply calculating the intensities of these images, we arrive at quadratic fringes:

$$p_1 + p_2 - p_3 - p_4 = A_s \sin \alpha(x, y), \qquad (6)$$

$$p_1 - p_2 + p_3 - p_4 = A_c \cos \alpha(x, y). \qquad (7)$$

Amplitudes A_s and A_c possess equal value under the conditions that[13] $z = 2.45$ rad and $\theta = 56°$. The z

value can be precisely determined from the ratio be-
tween the first and the third harmonics of the inter-
ference signal detected by the PD.[14] Phase $\alpha(x, y)$ is
given by

$$\alpha(x, y) = \tan^{-1}\left(\frac{p_1 + p_2 - p_3 - p_4}{p_1 - p_2 + p_3 - p_4}\right). \quad (8)$$

In a variation of the technique outlined above, a si-
nusoidal modulating current is injected into the LD,
as shown in Fig. 3(b). During period T1, current
flow is channeled to LD1. When they are viewed by
a CCD camera, interference fringes $S_1(t, x, y)$ and
$S_2(t, x, y)$ can be seen to overlap, because bias cur-
rents are injected into both LDs. All images p_{2k} ($k =$
1–4) detected with respect to LD2, however, are the
same. At this point we can detect only $\sin \alpha_1(x, y)$
and $\cos \alpha_1(x, y)$ by using Eqs. (6) and (7) because
these calculations give zeros for the same images.
In contrast, because there is no modulating signal
where LD1 is concerned, images P_{ik} ($k = 5$–8) are the
same during period T2. Then we can obtain only
$\sin \alpha_2(x, y)$ and $\cos \alpha_2(x, y)$. That is, the quadratic
fringes are obtained only for a sinusoidal phase-
modulated LD.

C. Step-Height Measurement

Step height is calculated by means of traditional two-
wavelength interferometry. The difference between
$\alpha_1(x, y)$ and $\alpha_2(x, y)$ is given by

$$\Delta\alpha(x, y) = \alpha_1(x, y) - \alpha_2(x, y) = 4\pi L(x, y)/\Lambda, \quad (9)$$

where

$$\Lambda = \lambda_1\lambda_2/|\lambda_1 - \lambda_2| \quad (10)$$

is a synthetic wavelength.

When $L(x, y)$ is larger than one half of one wave-
length, the unwrapped phase $\widehat{\alpha}(x, y)$ is expressed by

$$\widehat{\alpha}_1 = \alpha_1(x, y) + 2n\pi, \quad (11)$$

where n is an integer. From Eqs. (4), (9), and (11),
$L(x, y)$ is calculated as[15]

$$L(x, y) =$$
$$\frac{\lambda_1\{\alpha_1(x, y) + 2\pi \, \text{INT}[R\Delta\alpha(x, y) - \alpha_1(x, y)]/2\pi\}}{4\pi}, \quad (12)$$

wherein $R = \Lambda/\lambda_1$ represents the ratio of the syn-
thetic wavelength to that of the LD and the function
INT[ ] gives the integer of the argument.

3. Experimental Setup

In the experimental setup shown in Fig. 1 the wave-
lengths of LD1 and LD2 were 685 and 785 nm, re-
spectively. Synthetic wavelength Λ became 5.38
μm. The test surface shown in Fig. 2 consists of
gauge blocks (Mitutoyo). Gauge blocks 1 and 2 are
attached to gauge block 3 by atmospheric pressure.
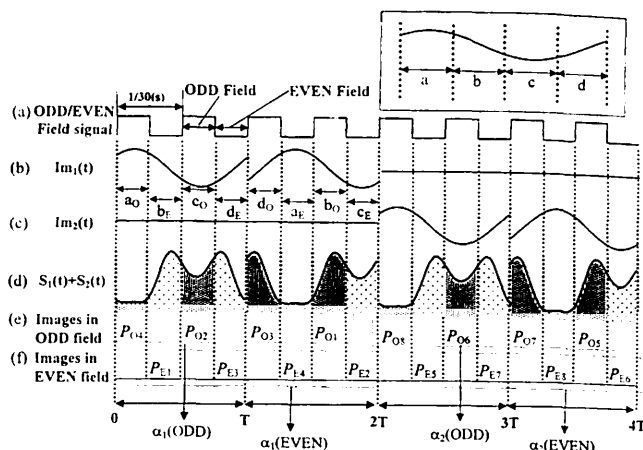Gauge blocks 1, 2, and 3 have thicknesses of 1, 1.001,

Fig. 4. Timing chart of the modulation process in the experiment.

and 10 mm within tolerances provided by the manu-
facturer of 0.03, 0.02, and 0.06 μm, respectively.
The optical path difference was 100 mm. The com-
bined interference fringe is magnified three times by
lenses L1 and L2, and the image is captured by a CCD
camera whose pixel size and count are 6.35 μm $\times$
7.40 μm and 768 (horizontal) $\times$ 494 (vertical), respec-
tively. As the output video signal of the CCD cam-
era used in our experiment is based on the National
Television System Committee standards, the frame
rate is 30 Hz. The video signal from this device is
fed to the video-capture board, allowing the phase
distribution to be calculated from Eq. (12). As the
modulation depths in both signals was 2.45, the am-
plitude of the modulating current was ~0.4 mA for
both LDs. We neglected intensity modulation be-
cause the modulation currents were sufficiently
small. The precise timing of the modulating process
is shown in Fig. 4, in which Figs. 4(a)–4(e) correspond
directly to the same designations in Fig. 1. Because
images that correspond to even or odd fields are de-
tected by turns, in general-purpose CCD cameras a
special modulating signal is required for detection of
the four images for calculating Eqs. (6) and (7). Sig-
nal processing as shown in Fig. 4 enables us to cal-
culate phase distributions in both fields. This
means that we can retain the spatial resolution orig-
inally provided by the CCD camera. As the even–
odd cycle continues as shown in Fig. 4(a), two periods
of sinusoidal modulating signals are injected into one
LD. The phases of the modulating signals, $\text{Im}_1(t)$
and $\text{Im}_2(t)$, which are shown in Figs. 4(b) and 4(c),
respectively, are changed by $\pi/2$ at T and $3T$. In-
terference images overlap as shown in Fig. 4(d). An
image must be detected at each of the four sections
shown in the inset of Fig. 4. These sections corre-
spond to a_O–d_O and a_E–d_E, respectively, as shown in
Fig. 4(b). Subscripts O and E represent odd and
even fields, respectively. Four images P_{Ok} ($k = 1$–4)
that correspond to the odd field are obtained in the
periods a_O, b_O, c_O, and d_O, as shown in Fig. 4(e).
Phase $\alpha_1(\text{ODD})$ in the odd field is calculated by use of
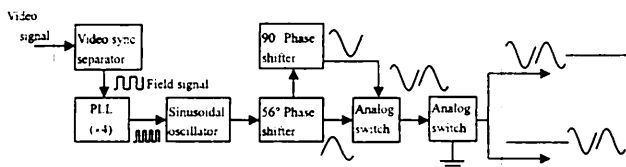these four images. In the period from $2T$ through

Fig. 5. Block diagram of the modulating-signal generator.

4T, phase α_2(ODD) is derived from P_{Ok} (k = 5–8). In the same manner, phases α_1(EVEN) and α_2(EVEN) are derived from P_{Ek} (k = 1–4) and P_{Ek} (k = 5–8), respectively, as shown in Fig. 4(f). Therefore the step height is obtained by use of Eq. (12).

A schematic of the modulating-signal generator is shown in Fig. 5. The ODD–EVEN field signal is separated from the video signal and then fed into the phase-locked loop (PLL) to increase the number of cycles by four times. An oscillator that has an input terminal for an external sync signal generates a sinusoidal signal, which remains synchronous with the field signal. The frequency of the sinusoidal signal is 7.5 Hz because calculations from Eqs. (6) and (7) require four frames of the video signal. The initial phase of the sinusoidal signal is adjusted to 56° by the phase shifter to achieve the condition required for the

calculation of Eq. (8). Another phase shifter shifts the phase of this signal by 90°. Two sinusoidal signals are mixed in the first analog switch to generate the required modulating signal. The second switch manages the time-sharing modulation.

4. Results

Figure 6 shows examples of the captured images and the separate quadratic fringes. Images P_{O1}–P_{O8} shown in Fig. 6(a) are obtained in the odd field. They correspond to those with the same designations in Fig. 4(e). Visibilities in P_{O2} and P_{O6} are especially poor because of overlap. The quadratic fringes, however, are clearly separated by use of the calculations of Eqs. (6) and (7), as shown in Figs. 6(b) and 6(c), respectively. The phase of the cosine fringe differs by 90° from that of the sine fringe. Also, the period of the fringe in Fig. 6(b) is smaller than that in Fig. 6(c). These results confirm the effectiveness of the proposed technique.

We measured the surface profile of the plane mirror by employing only LD1 to confirm the measurement accuracy of the optical setup. The result is shown in Fig. 7. The measurement error was estimated to be 15 nm rms. We believe that the source of the error is mainly mechanical disturbances.
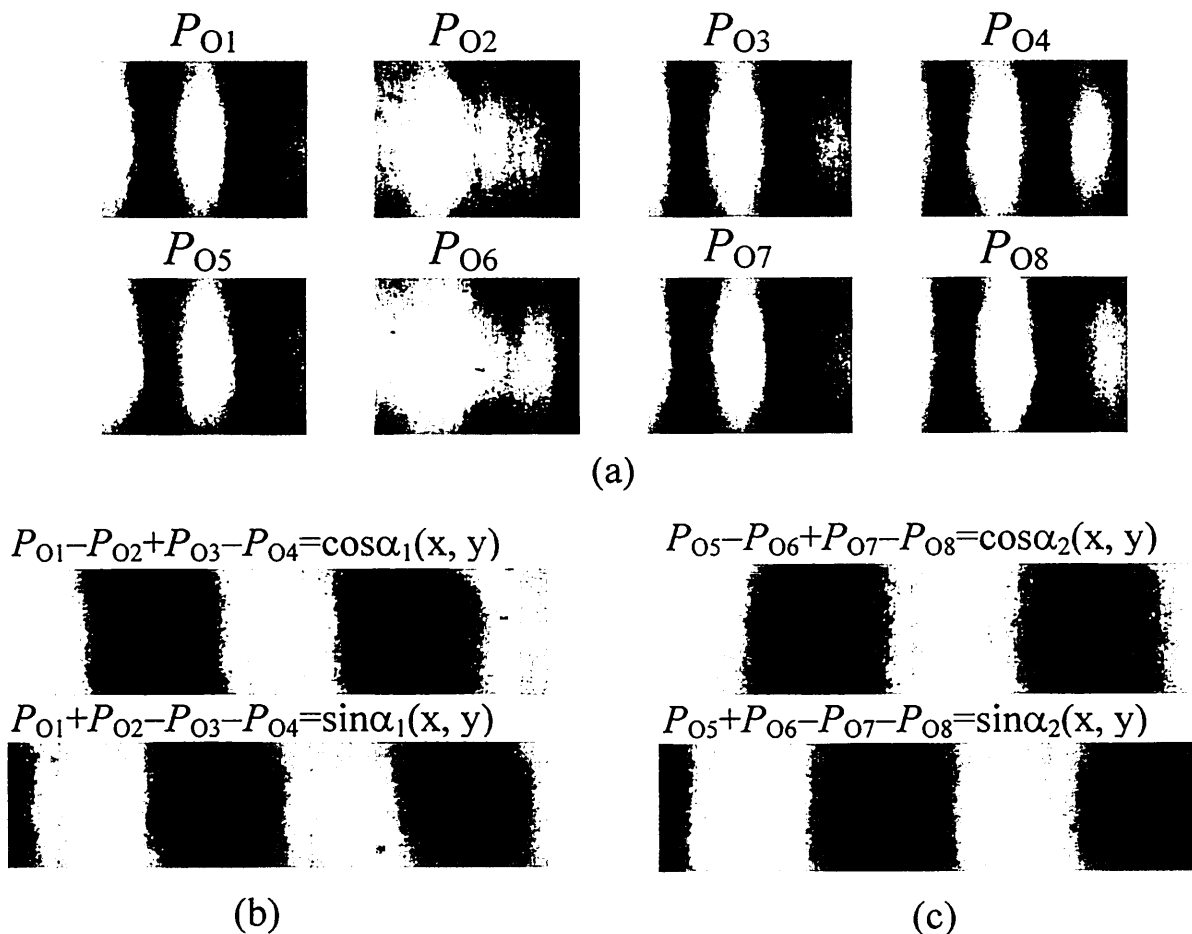

(a)

$P_{O1}-P_{O2}+P_{O3}-P_{O4}=\cos\alpha_1(x, y)$

$P_{O1}+P_{O2}-P_{O3}-P_{O4}=\sin\alpha_1(x, y)$

(b)

$P_{O5}-P_{O6}+P_{O7}-P_{O8}=\cos\alpha_2(x, y)$

$P_{O5}+P_{O6}-P_{O7}-P_{O8}=\sin\alpha_2(x, y)$

(c)

Fig. 6. Fringes (a) captured with the CCD camera, (b) calculated for λ_1, and (c) calculated for λ_2.
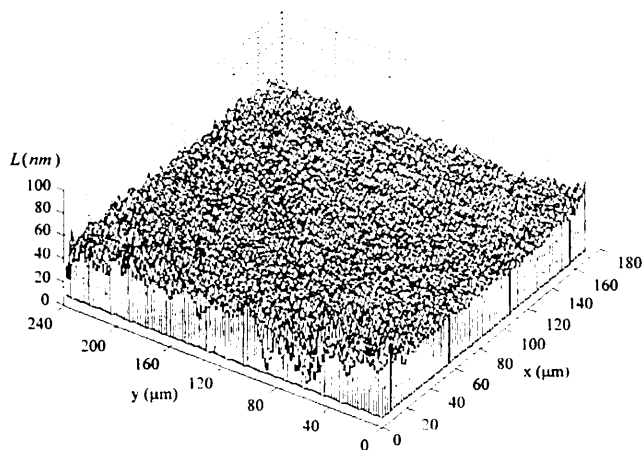
Fig. 7. Surface profile of the flat mirror measured with a single wavelength.
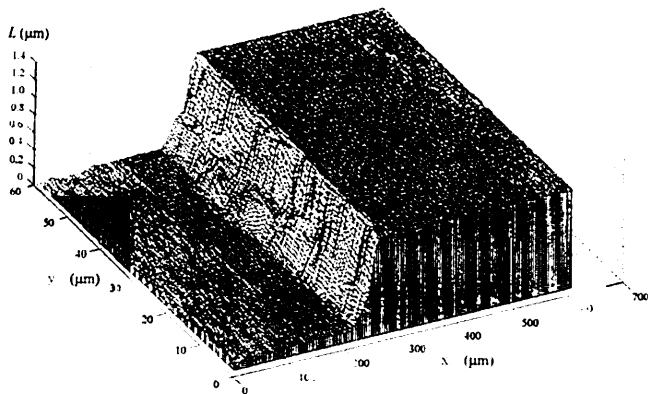

Fig. 8. Result of the step-height measurement.

This error can be reduced if a feedback control is added to the design.[16]

Figure 8 gives the results of our step-height measurement. The figure applies to the even and the odd fields. A step height of 1 μm made with gauge blocks was detected. We spatially averaged this result for all the measurement areas with a low-pass filter to reduce the spike noise that was generated by unexpected reflections near the boundaries between gauge blocks. The measurement error was estimated to be within 15 nm rms in this instance, as measured by a flat mirror.

5. Conclusions

A TWI that uses the integrating-bucket method in conjunction with a new modulating technique has been proposed. Time-shared sinusoidal phase mod-

ulation enables us to obtain the integrated interference fringes required for phase calculation. Quadratic fringes can be clearly separated, and a step height of 1 μm with an error of ≤15 nm rms was measured. It should be possible to reduce this error further by addition of a feedback control.

References

1. J. C. Wyant, "Testing aspherics using two-wavelength holography," Appl. Opt. 10, 2113–2118 (1971).
2. C. Polhemus, "Two-wavelength interferometry," Appl. Opt. 12, 2071–2074 (1973).
3. K. Creath, "Step height measurement using two-wavelength phase-shifting interferometry," Appl. Opt. 26, 2810–2816 (1987).
4. G. Beheim, "Fiber-optic interferometer using frequency-modulated laser diodes," Appl. Opt. 25, 3469–3472 (1986).
5. A. J. den Boef, "Two-wavelength scanning spot interferometer using single-frequency diode lasers," Appl. Opt. 27, 306–311 (1988).
6. Y. Ishii and R. Onodera, "Two-wavelength laser-diode interferometry that uses a phase-shifting technique," Opt. Lett. 16, 1523–1525 (1991).
7. Z. Sodnik, E. Fischer, T. Ittner, and H. J. Tiziani, "Two-wavelength double heterodyne interferometry using a matched grating technique," Appl. Opt. 30, 3139–3144 (1991).
8. R. Onodera and Y. Ishii, "Time-multiplex two-wavelength heterodyne interferometer with frequency-ramped laser diode," Opt. Commun. 167, 47–51 (1999).
9. O. Sasaki, H. Sasazaki, and T. Suzuki, "Two-wavelength sinusoidal phase/modulating laser-diode interferometer insensitive to external disturbances," Appl. Opt. 30, 4040–4045 (1991).
10. T. Suzuki, K. Kobayashi, and O. Sasaki, "Real-time displacement measurement with a two-wavelength sinusoidal phase-modulating laser diode interferometer," Appl. Opt. 39, 2646–2652 (2000).
11. R. Onodera and Y. Ishii, "Two-wavelength interferometry that uses a Fourier-transform method," Appl. Opt. 37, 7988–7994 (1998).
12. O. Sasaki, H. Okazaki, and M. Sakai, "Sinusoidal phase modulating interferometer using the integrating-bucket method," Appl. Opt. 26, 1089–1093 (1987).
13. T. Suzuki, O. Sasaki, J. Kaneda, and T. Maruyama, "Real-time two-dimensional surface profile measurement in a sinusoidal phase modulating laser diode interferometer," Opt. Eng. 33, 2754–2759 (1994).
14. O. Sasaki and H. Okazaki, "Sinusoidal phase modulating interferometry for surface profile measurement," Appl. Opt. 25, 3137–3140 (1986).
15. T. Suzuki, H. Nakamura, and O. Sasaki, "Small-rotation angle measurement using an imaging method," Opt. Eng. 40, 426–432 (2000).
16. T. Suzuki, T. Maki, and O. Sasaki, "High-speed sinusoidal phase modulating laser diode interferometer with a feedback control to eliminate external disturbance," in International Symposium on Optical Engineering for Sensing and Nanotechnology, K. Iwata, ed., Proc. SPIE 4416, 392–396 (2001).